

Investigations on Decreased High Temperature Ductility of Different Continuously Cast Steel Grades

Carolin Fix,* Lukas Borrmann, Sina-Maria Elixmann, Carolin Grahe, Svenja Kurenbach, and Dieter Senk*

Dedicated to Professor Wolfgang Bleck on the occasion of his 70th birthday.


Continuous casting of premium steel grades requires a process with a high degree of precision and the knowledge about the mechanical behavior of the steel at temperatures above 800 °C. Herein, several origins of effects which lead to unwanted impairment of the hot strand shell like segregations, size, amount, kind, and distribution of precipitates as well as porosities from a metallurgical point of view are dealt. The systematic description of potential defect reasons helps to predict harmful operation parameters in context with the chemical composition of steel grades. A compilation of results from experiments at Department of Ferrous Metallurgy of RWTH Aachen University is complemented by a literature review. It is focused on the high temperature ductility and the underlying mechanisms inside the solidifying steel. Finally, potential measures to adjust the continuous casting process to prevent defects are elaborated.

1. Introduction

Steel design for new grades aims on improvement of several steel properties like strength, ductility, formability, and premium surface conditions at the same time. Those goals can be achieved by sophisticated micro, low, or high alloying of steels, controlled solidification and thermomechanical treatment during the subsequent process steps. Melt treatment and solidification in particular play important roles for the further steel properties.

C. Fix, L. Borrmann, S.-M. Elixmann, C. Grahe, S. Kurenbach, D. Senk
Steel Institute IEHK
Chair of Metallurgy of Iron and Steel
Intzestraße 1, Aachen 52072, Germany
E-mail: carolin.fix@iehk.rwth-aachen.de;
dieter.senk@iehk.rwth-aachen.de

C. Fix
Rheinisch-Westfälische Technische Hochschule Aachen
Ferrous Metallurgy
Intzestraße 1, Aachen 52072, Germany

 The ORCID identification number(s) for the author(s) of this article can be found under <https://doi.org/10.1002/srin.202100323>.

© 2021 The Authors. Steel Research International published by Wiley-VCH GmbH. This is an open access article under the terms of the Creative Commons Attribution License, which permits use, distribution and reproduction in any medium, provided the original work is properly cited.

DOI: 10.1002/srin.202100323

This relation results from micro-, semi-, and macrosegregation influencing the element distribution inside the casting semi.

In continuous casting machines, cooling of the strand influences the solidification and thus the high temperature properties of steel grades. The strand shell develops as a network of mainly columnar dendrites. Adjacent dendrites grow and naturally weld together when the residual liquid layers solidify forming a weight bearing strand shell. Already during solidification nonmetallic precipitates are formed and diminish the ductility in the high temperature range.

Due to thermal and mechanical stresses in continuous casting machines, defects like cracks can be expected. With knowledge of temperatures where the steel is

associated with brittle behavior, the danger of crack formation can be estimated and reduced. By means of further explorations and modelling, countermeasures against defects can be significantly improved.

Since several decades the Department of Ferrous Metallurgy at RWTH Aachen University investigates solidification-related mechanisms among others using in situ hot tensile tests. In this article, the particular weakening effects on the hot steel specimen are described based on results from hot ductility investigations. A comprehensive summary of literature is given, supplemented by new results from the IEHK, including so far unpublished results from German Common Research Center “SFB761-Steel ab initio” and ongoing RFCS-project “PMAPIA.”

It is distinguished between internal factors like the chemical compositions, which can only be influenced in narrow ranges to meet the material requirements, and the external parameters, that summarize the casting conditions. Focusing on the hot ductility behavior and the related surface and subsurface crack formation in continuous casting, the characteristic phenomena at relevant temperature regions are described.

2. Experimental Setups to Identify High Temperature Mechanical Properties

The ductility of new steel grades is usually determined by hot tensile tests. Thereby, three thermal strategies could be differentiated, direct heating to test temperature, annealing

aforementioned test temperature, and in situ, whereby the liquidus temperature was exceeded, e.g., at IEHK's continuous casting (CC) simulator. Nowadays, only the latter two methods were used, whereby only the in situ strategy maps effects such as grain coarsening, precipitation behavior, or hot cracking according to the CC process.^[1]

In Austria at MU Leoben testing methods as the “mold simulator” and the “submerged split-chill tensile test” (SSCT) were developed to determine and describe the ductility behavior under CC similar conditions.^[2,3] In addition, there were various high temperature bending methods which investigate the strain, the frequency of crack formation, and the maximal crack length.^[4–7]

Torsion and compression tests were also used to determine critical strains.^[8,9] To investigate mechanical loads during solidification as well as hot tearing, the high temperature bending simulator was developed at the IEHK. This enabled the deformation of the ingot shell with liquid core, whereas force and displacement data were recorded. Alloy-specific characteristic values for the compressive load were determined in hot compression tests.

3. Reduction of Cross-Sectional Area and Ductility Influencing Factors

To prevent internal and surface cracking in continuous casting of steel, it is essential to understand the mechanisms in the steel during solidification and cooling. Complex interactions between alloy composition, and external conditions like cooling rate and strain rate are proven to have a great impact on each steel, individually.

Hot tensile tests to obtain the ductility are inter alia evaluated in terms of the relative reduction of area RA (%) of the specimen's cross section. **Figure 1** shows the effect of changes in the

steel itself differentiated in temperature ranges on the RA according to the recent results of research at the IEHK. Two^[10,11] or three,^[12] respectively, low ductility zones LDZ of composition-dependend emphasis can be identified. LDZ1 describes the temperature range before the steel reaches its maximum ductility at the point T_{BD} , the temperature of the brittle–ductile transformation. LDZ1 is mainly influenced by the degree of solidification, as this determines whether the dendritic crystals are already firmly connected. At the zero-strength temperature, the adjacent dendrites meet this criterion for the first time resulting in the material being able to bear a small load but being still too weak to deform before failing. There is controversial information on T_{sol} being either higher than the zero-ductility temperature (ZDT),^[10,13–15] or slightly lower.^[2] For peritectic steel, grades were even found that the ZDT equals the ZST if body-centred cubic δ -Fe is the first phase. The calculated f_s at this point was given with 0.8.^[16] Cracks, that occur in the LDZ1 and show a dendritic structure at the fracture surface, are referred to as “hot tearing.”^[17–19]

The LDZ2 defines the second temperature range where the ductility is impaired by mechanisms inside the steel, starting with the ductile–brittle transition at T_{DB} . In case, the deterioration starts because of the formation of secondary MnS or low melting FeS, it is referred to as LDZ2a, whereas LDZ2b is induced by the precipitation of nitrides. The material is the weakest when the transition from austenite to ferrite starts at primary austenite grain boundaries. A thin layer of ferrite makes the steel particularly vulnerable.^[20] After the phase transition, the materials' ductility recovers. Just like the evolving of ferrite, other phase transformations are impairing the ductility.

For the interpretation of these results, it must be noted that the testing method^[21–23] and the testing parameters have a significant influence on the materials' behavior. Variation of parameter

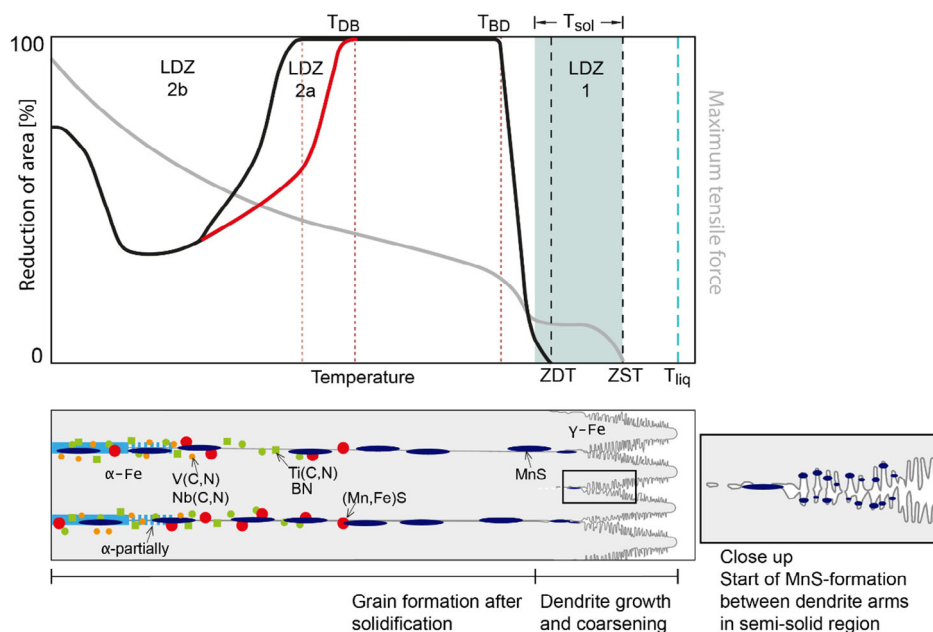


Figure 1. Schematic representation of RA curve for high temperature ductility, depending on: temperature, individual composition, formed precipitates, and phase transformations, representation based on data from literature.^[2,10,11,58,60]

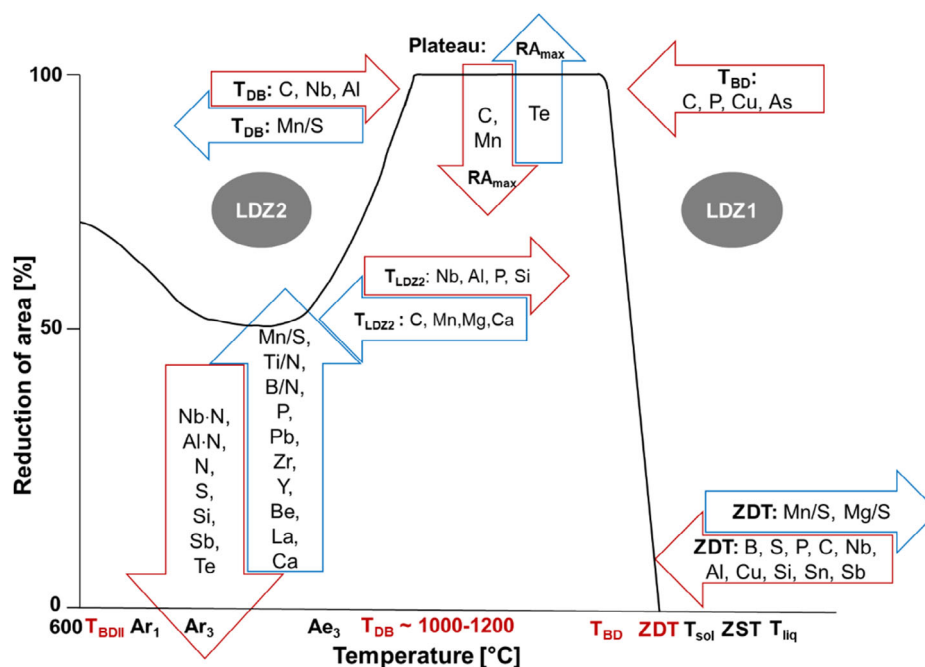


Figure 2. Qualitative representation of the influence of increasing contents of alloying elements on the hot ductility, blue: improvement, red: deterioration; data from literature.^[13,20,25,28–30,53,61–68] summarized by Unterberg.^[69]

sets^[20,24–28] in hot ductility testings thus provide important information on possible adjustments of the casting process to match the materials' properties.

Figure 2 shows the qualitative influence of various alloying elements. Ratios and products of alloying elements, that form a joint precipitated which affects the ductility are considered. Nitrogen alone is mostly found to have no harmful impact, but Al- and Nb nitrides have.^[29,30] ratios Mn/S, Ti/N, and B/N are included, because a stoichiometric ratio of these alloying elements, prevent the formation of precipitates that have a strong negative impact on the hot ductility, if exceeded. A sufficient Mn content protects the formation of low melting (Fe,Mn)S, whereas TiN and BN bind the nitrogen resulting in inhibited AlN formation at lower temperatures.

3.1. Segregation

Segregation is caused by different solubilities of alloying elements in the liquid steel and the solid matrix. Rejection of elements from the solid phase leads to an increase in the residual melt and consequently to a positive microsegregation.^[31–33] The primary solidification in steel castings can be columnar dendritic, equiaxed dendritic, or globular, depending on the boundary conditions.^[34–37] During dendritic solidification, the microsegregated melt gets captured between the dendritic arms. As globulites have a round shape and no branches, this structure provides bigger coherent area. Caused by this geometric effect, a mesosegregation, which is larger than microsegregation, can be found (**Figure 3**).

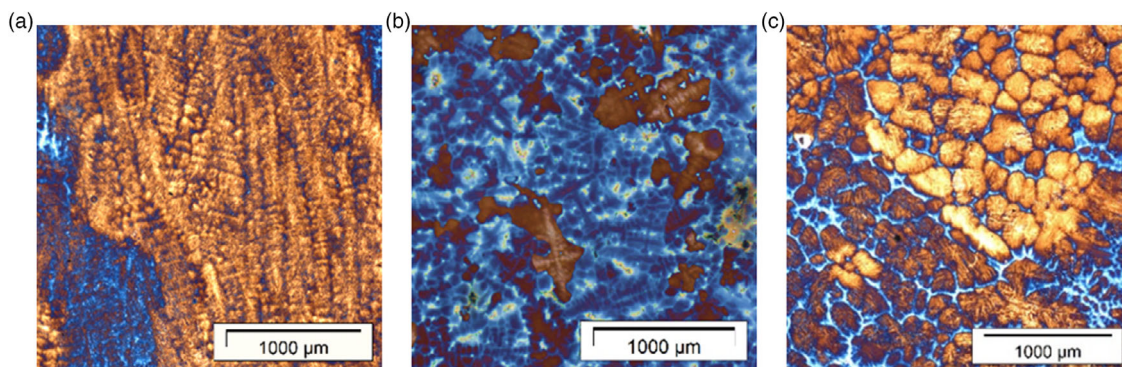


Figure 3. Different solidification structures, examples show medium and high manganese steels, light optical microscopy, a) columnar dendrites, b) equiaxed dendrites, and c) globular structure. Reproduced with permission.^[70] Copyright 2019, VDEh.

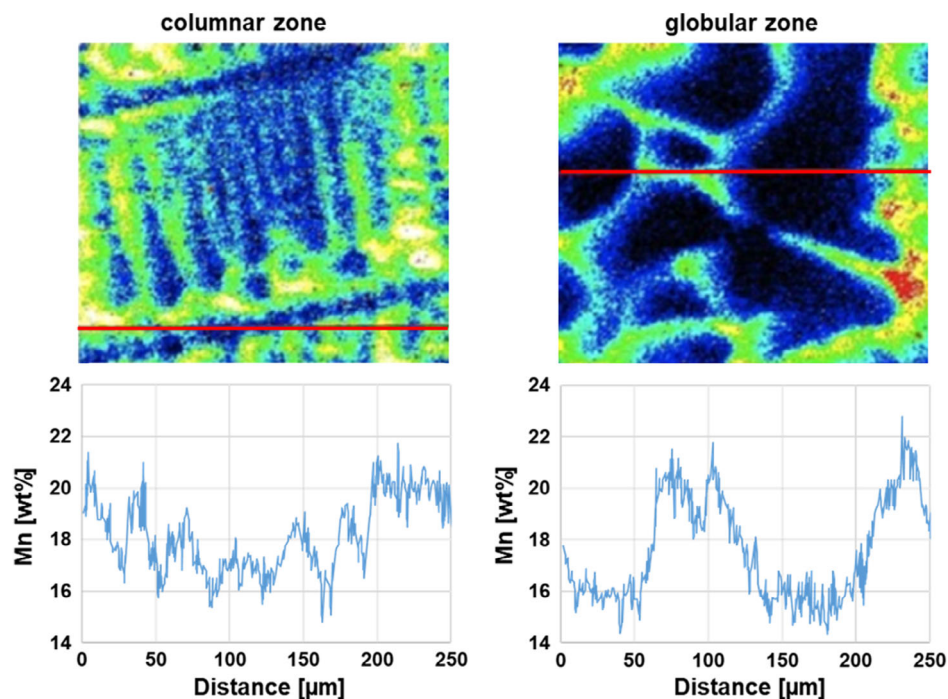


Figure 4. EPMA measurement of microsegregation in different as-cast structures of high manganese steels left: [Mn] = 18.4 wt%, right: [Mn] = 19.9 wt%. Reproduced with permission.^[71] Copyright 2017, ASMET.

The line scans in **Figure 4** clearly show the relationship between the as-cast structure and the resulting microsegregation distribution and intensity.

This can in turn have a major impact on the microstructure development, as **Figure 5** underlines by showing the microstructure after reheating and a hot compression test of a high manganese steel. Thus, different concentrations are present in a relatively small sample area, which significantly influence the microstructure and its transformation during cooling and deformation, creating narrow bands of adjacent different phases. The brownish areas represent the former dendrite stems in which a temperature-induced martensitic substructure is present, which

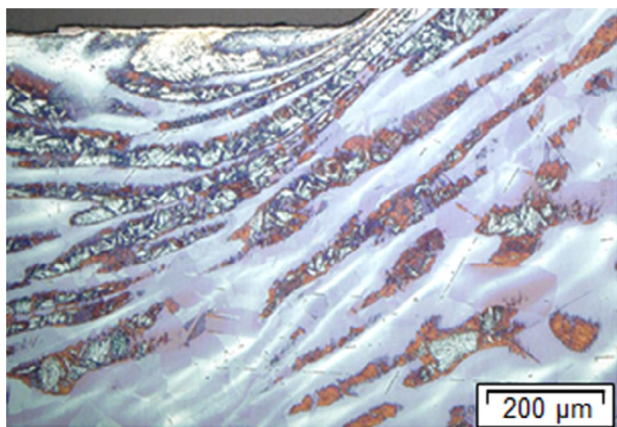


Figure 5. LOM of ×30 MnAl17-1 after hot compression test at 1300 °C with $\varphi = 0.3$ and $\dot{\varphi} = 5 \text{ s}^{-1}$.

is only possible due to the decrease in Mn and C as well as an increase in Al concentration. This effect can be explained by Equation (1) for martensite start temperature from Hollomon et al.,^[38] which shows the impact of the elements.^[39] The remaining light blue/purple areas are to be interpreted as Mn-rich austenite.

$$M_{S1}[^{\circ}\text{C}] = 550 - 350(\% \text{C}) - 40(\% \text{Mn}) - 35(\% \text{V}) \\ - 20(\% \text{Cr}) - 17(\% \text{Ni}) - 10(\% \text{Cu}) - 10(\% \text{Mo}) \\ - 8(\% \text{W}) + 15(\% \text{Co}) + 30(\% \text{Al}) \quad (1)$$

Microstructure examinations of tested hot tensile specimens show, that the ductile deformation results in microstructural banding as well (**Figure 6**). Banding is observed for aluminum and manganese, whereby the enriched bands of Mn and Al alter, as Al segregated in the crystals solidifying first, whereas Mn enriches in the residual liquid.

Segregation, which is rather caused by the casting process than by the solidification structure, is called macrosegregation. The process leads to fluid flows that concentrate the microsegregated melt in the middle part of the casting semi.^[34,40,41] This mechanism can be suppressed or mitigated either by applying mechanical or thermal soft reduction or a change of the as-cast structure by electromagnetic stirring.^[37,42–45]

3.2. Precipitates

Precipitates are secondary, nonmetallic phases which form due to a local exceedance of the solubility product. Thus, they are directly depending on the local concentrations and therefore

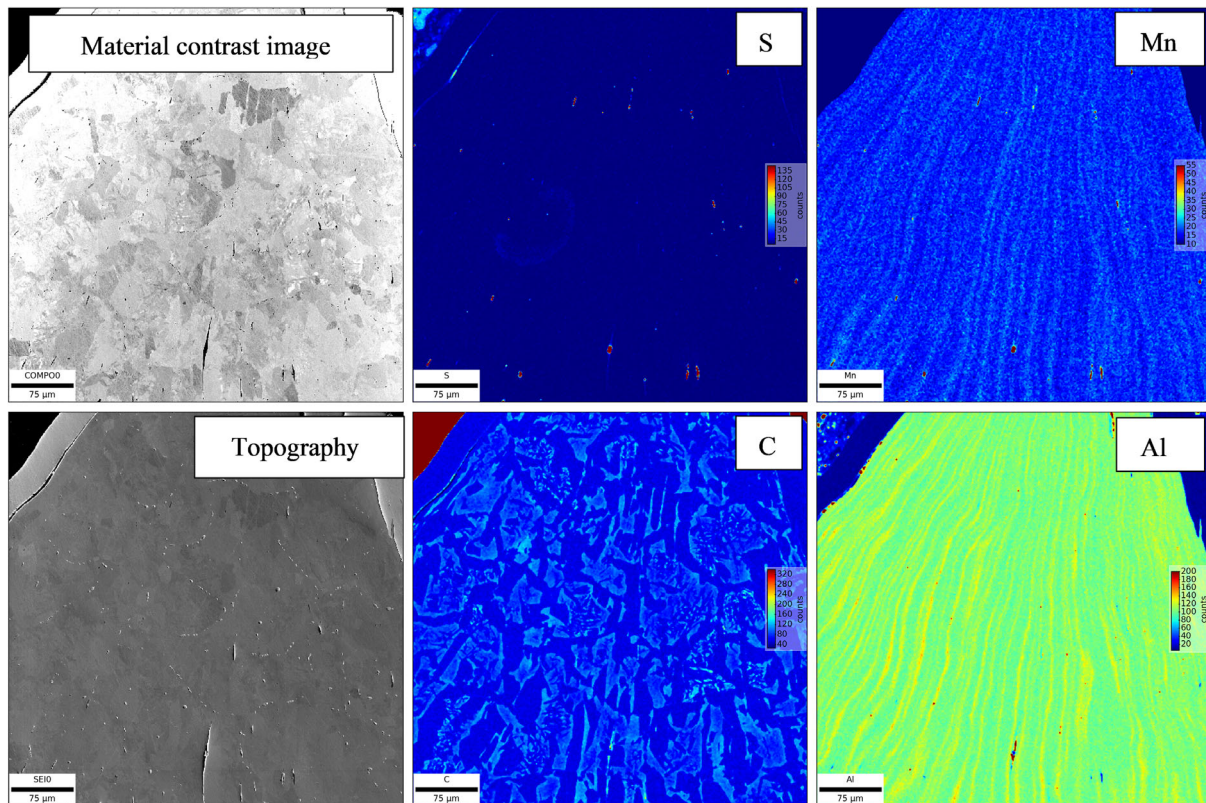


Figure 6. EPMA analysis of a hot tensile specimen tested at $T=1100\text{ }^{\circ}\text{C}$, 100% RA, showing microstructural banding of Mn and Al; qualitative representation of element distribution, $[\text{C}]=0.18\text{ wt\%}$, $[\text{Mn}]=1.7\text{ wt\%}$, $[\text{S}]=0.014\text{ wt\%}$; $[\text{Al}]=1.4\text{ wt\%}$.

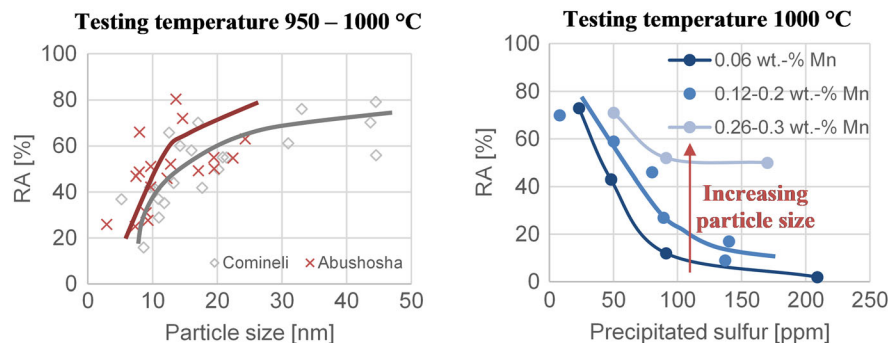


Figure 7. Examples for quantified influencing factors on the RA in LDZ2, left: increasing particle size in Ti-containing steels beneficial for hot ductility,^[46,47] right: decreasing amount of precipitated S and increasing Mn content improve the ductility in low C steel with 0.03–0.05 wt% C.^[48]

from the chemical composition (internal parameter), cooling rate (external parameter). **Figure 7** shows exemplary two quantifications of influencing factors on the RA in the temperature range of the second ductility minimum LDZ2. An increase in the particle size clearly leads to a great improvement of the hot ductility and indicates that the finer the particles are, the more significant is their influence on the ductility.^[46,47] The right diagram shows how a reduction of the total amount of precipitating sulfur benefits the ductility at a testing temperature of $1000\text{ }^{\circ}\text{C}$, same applies to an increase in the Mn content. The higher Mn contents were found to shift the size distribution of the MnS to bigger

particles, whereas significantly lowering the amount of particularly small sulfides.^[48] That in turn fits well with the results from the left diagram and gives an idea of the complex interrelationships of various influencing variables.

The fact, that especially small precipitates are impairing the materials ability to resist loads or stresses, leads to a special sensitivity to surface and subsurface cracks in materials that are likely to produce a high number of small precipitates, like for example microalloyed steels. The particle size of the precipitates like TiN, AlN, Nb(CN), and MnS are dependent on the cooling rate. With a high cooling rate, the particle size decreases and it is

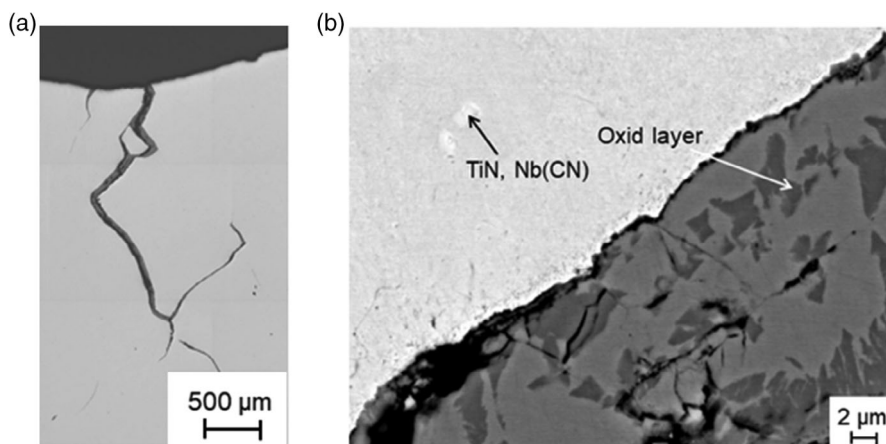


Figure 8. a) LOM of a transverse corner crack in an oscillation mark of a microalloyed steel slab and b) SEM-EDX analysis of the crack from a) with TiN and Nb(CN).

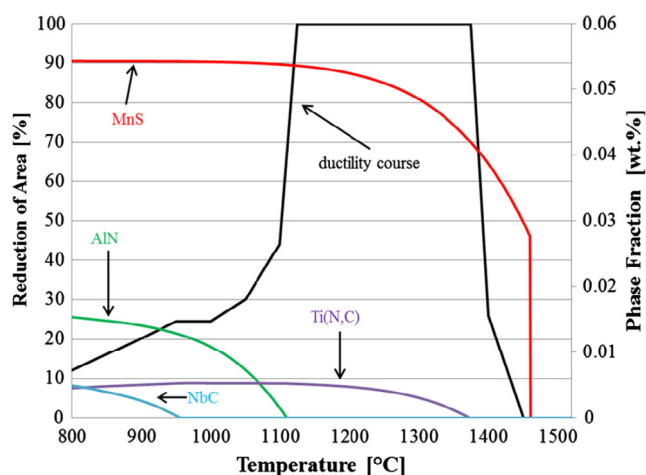


Figure 9. RA from hot tensile tests of a microalloyed steel grade and the related Thermo-Calc[®] calculations; the temperature of precipitate formation can be compared with the partially impaired ductility value. Reproduced with permission.^[25] Copyright 2015, Metall Mater Trans B.

easier for cracks to propagate along the chain of precipitates on the grain boundaries. Small precipitates at grain boundaries result in a pinning of the grain boundaries and thus lower the ductility. This effect is particularly pronounced in microalloying

steels, especially for Nb(CN) precipitates.^[22,23] Continuous casting employs a high cooling rate and a cyclical thermal load on the surface of the strand. Combined, the effects lead to an increased risk for transverse corner cracks in microalloyed steels.^[47,49] An example for a surface crack propagating along primary austenite grain boundaries in a microalloyed steel is shown in **Figure 8**. Small-scale precipitations were detected with SEM-EDX near the crack, which was filled with an oxide layer during cooling.

Thermodynamic calculation of the phase fraction of precipitates depending on the temperature can help to understand the reasons for an impaired hot ductility, as shown in **Figure 9**. Especially in the LDZ2, the drop of the RA is related to the formation of first AlN and second NbC, in particular due to the former explained effect of grain boundary pinning.

To monitor and validate the effects of the chemical composition, segregation, and the resulting precipitation behavior, the IEHK's slow solidification furnace is used to produce large crystals and nonmetallic inclusions. **Figure 10** shows precipitates of MnS and AlN as a result of this slow solidification process. Depending on the Al content present, the precipitation sequence results and the first formed phase serves as a heterogeneous nucleation surface for the subsequent phase. Thus, the chemical composition of the melt influences the chronological order when the solubility product $\log K_{[\%Mn][\%S]} = -17\,026/T + 5.161$ or $\log K_{[\%Al][\%N]} = -12\,950/T + 5.58$ is exceeded and thus the respective phase is precipitated.^[50,51] The solubility product is used

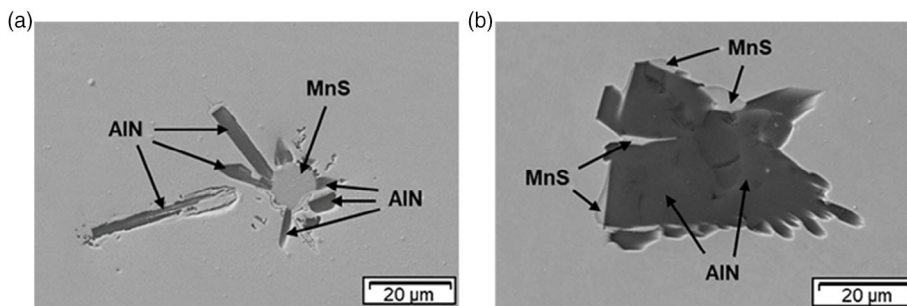


Figure 10. SEM-EDX analysis $\times 1000$ of a) X30MnAl17-1 and b) X30MnAl17-5; slow solidification process with a solidification speed of $\nu = 15 \text{ mm h}^{-1}$.^[72]

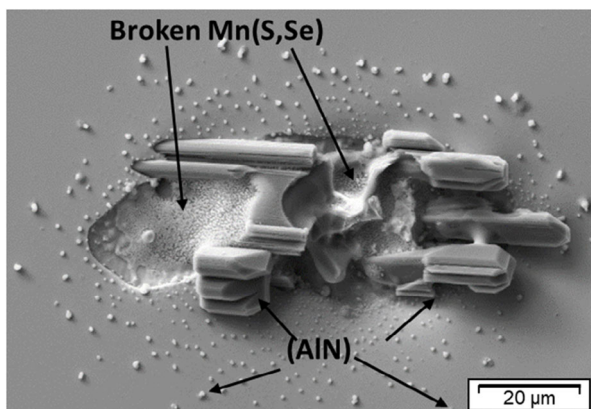


Figure 11. SEM-EDX analysis of X30MnAl17 3, $\times 1000$, complex (AlN) and Mn(S,Se) precipitation, and (AlN) in the initial stage of the formation process; slow solidification process with a solidification speed of $\nu = 15 \text{ mm h}^{-1}$.

as a base for thermodynamic calculation of steels to determine the precipitation sequence.

By etching the matrix, the structure of the precipitates in two-phase high manganese steels has been shown in three dimensions by SEM. In **Figure 11**, the nitrides exhibit a shell-like, fibrous growth; small punctiform precipitates ($< 1 \mu\text{m}$) can be seen around the complex precipitate. These dot-like precipitates are AlN in the initial stage. Due to the diffusion-driven depletion of [Al] and [N] of the residual melt forming this complex and due to the interdendritic separated areas during subsequent solidification, the precipitates do not have the possibility to coarsen and agglomerate with the complex precipitate.^[52]

3.3. Phase Transformations

Investigation of tensile strength peritectic steels show, that γ -Fe has a higher tensile strength than δ -Fe.^[16] In **Figure 12**, the influence of phase transformation in peritectic steels on the hot ductility behavior and the maximum tensile force are compared for different carbon contents. All compositions have in common,

that the maximum tensile strength is strongly influenced by the present phase. If γ -Fe is absent, F_{max} is low, but as soon as γ -Fe forms, a significant increase in the maximum tensile strength can be noted. The second observation concerns the effect of the phase-transformation on the reduction of area. In temperature ranges, where more than one phase is present, the ductility never reaches its maximum, and the ZDT is always lower than the T_{sol} .^[13] The softness of δ -Fe is not hindering the steel from reaching its maximum ductility, but the δ - γ -transformation leads to a local strain concentration in the δ -phase.

In LDZ2, the γ - α -phase transformation start with the precipitation of fine ferrite films at prior austenite grain boundaries. These thin layers of ferrite strongly impair the ductility; material recovers when ferrite films are thicker. The lower ductility results from the ferrite being the softer phase, wherefore the strain locally concentrates there. Thin bands of ferrite may occur at higher temperatures than A_{r3} and reach temperatures up to A_{e3} due to the transformation being strain induced.^[53]

3.4. Porosity

Porosity also should be considered evaluating hot ductility test results. Before testing, the specimen rod is melted completely in a zone. In this process, the diameter is increasing up to the diameter of the crucible. This increased volume at constant mass could lead to higher amounts of porosity (**Figure 13**) which is reducing the force bearing area and therefore the maximum reachable ductility. Porosity in general is known to reduce the mechanical properties, e.g., the Young's modulus and shortens the fatigue life. In continuous casting, porosity in the strand shell increases the breakout probability, too.^[54–57]

Different types of porosity can be defined. **Figure 14** shows a classification of porosity origins. A main differentiation is made between gas- and solidification-induced porosity.

Gas porosity may form by the recombination of dissolved gases or can be induced by stopper gas at the SEN in CC, such as argon or nitrogen. **Figure 15** shows a shrinkage pore with a MnS precipitation. This picture illustrates that even if pores are closed in further processing, e.g., by hot rolling, the precipitates

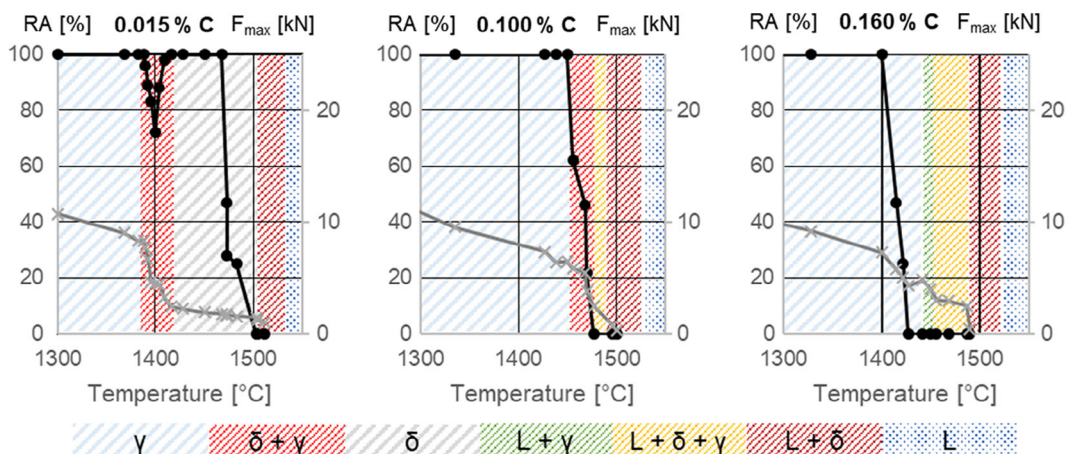


Figure 12. Influence of phase transformation at high temperatures in peritectic steels on ZST, ZDT, RA_{max} , and maximum tensile force F_{max} (kN), that is needed to keep a constant strain rate. Reproduced with permission.^[13] Copyright 1980, Wiley-VCH.

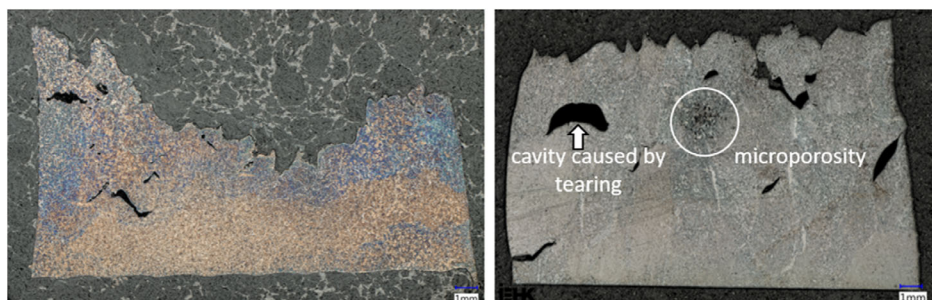


Figure 13. Porosity beneath the fracture area of different steel grades at 850 °C.

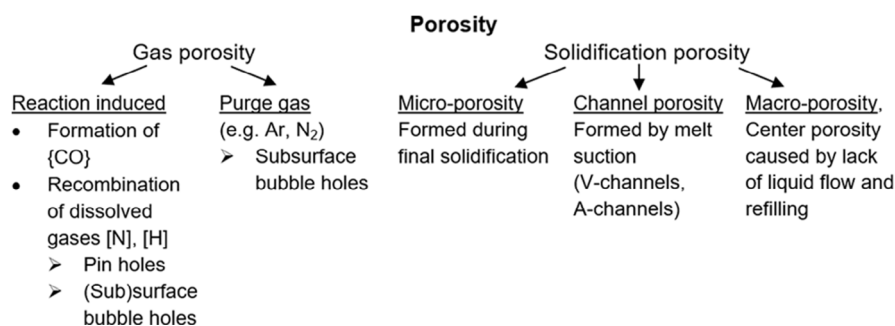


Figure 14. Classification chart for porosity formation.^[35,73–81]

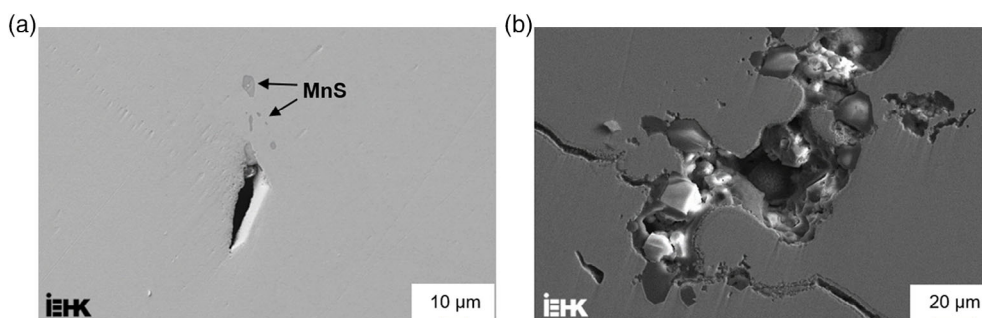


Figure 15. SEM-EDX analysis of a) shrinkage pore in as-cast structure with MnS precipitates and b) pores with cracks.

they contain remain and represent a flaw in the matrix. Precipitates even might be sucked into the pore caused by a local vacuum during pore formation. This can lead to a higher concentration of precipitates by movement of microsegregated melt seen in Figure 15b. The figure also presents different kinds of shrinkage porosity. Figure 15a shows shrinkage porosity in the solid phase (sharp edges) and in Figure 15b, shrinkage porosity is highlighted where some liquid has been present at final solidification (round edges).

Figure 16 shows two more examples of shrinkage porosity. Figure 16a shows an interdendritic pore (round shapes) and Figure 16b in the upper left side shows shrinkage at the grain boundaries.

To determine and understand which porosity leads to which weaknesses further research needs to be carried out.

4. Conclusions and Measures Against Decreased Ductility

To avoid decreased ductility ranges in critical CC plant positions, internal and external parameters need to be adjusted. The ductility of steel grades is influenced by various factors, such as steel composition, grain boundary development, thermal history, and strain rate.^[58] The described internal phenomena have to be systematically coordinated with the process to achieve the optimum properties of the casting semi.

Considering the chemical composition first, some alloying elements have a more detrimental impact than others. For example, ductility can be significantly improved by adjusting the Al, Nb, or N content, as well as by setting the optimum Mn/S ratio.^[25]

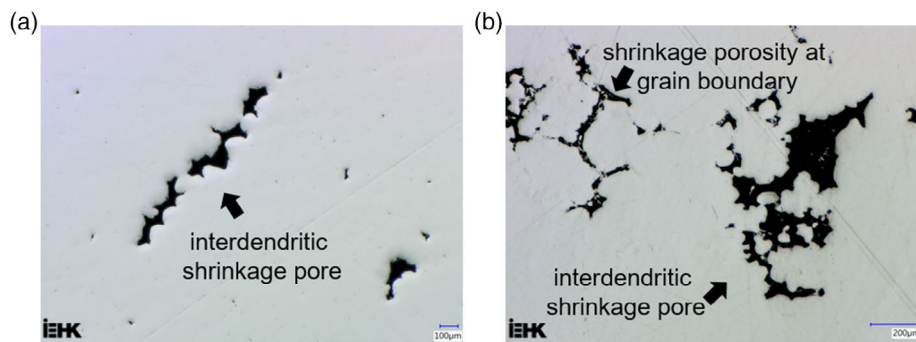


Figure 16. LOM of shrinkage porosity a) interdendritic and b) at grain boundary and interdendritic.

These elements can lead to an increased rate of fine precipitates, which are often the origin of cracks. An example of a damaging nitride is shown in Figure 8. However, sulfides or carbides can also act as crack initiators.

The effect of small changes of phase fractions during cooling can be estimated using thermochemical calculations, as shown in Figure 9. As well as the precipitates, phase transformations impair the RA curve at characteristic areas.

Knowledge of the precipitation formation in the as-cast structure and the areas of phase transformation of the specific steel compositions are an important input to individually set the optimum external parameters in casting process. This consideration is crucial to control the materials' properties with a tailored cooling strategy. Therefore, considering the temperature history is an essential step, especially of the surface region. Bending and unbending points are particularly critical areas of the continuous caster.^[59] Combined, these factors ensure that the material can resist the stresses even in regions with high strains. Less harmful precipitates in terms of formation temperature, size, number, and shape can be achieved by adjusting the process parameters.^[47]

In the end, the overall process should be safely controlled by analyzing the solidification properties of the casted material at different temperatures.

It has to be noted, that the adjustment of parameters can, at the same time, have beneficial effects on the LDZ1 by increasing the ZDT and lead to a worse ductility in the LDZ2.^[27]

5. Summary and Outlook

Various methods to analyze high temperature mechanical behavior were summarized. By these investigations the effects of steel composition and as-cast structure on ductile or brittle temperature ranges are determined. Segregation, precipitation of nonmetallic particles, phase transformation, and porosity are origins of brittleness during solidification and cooling. Inhomogeneities, especially fine-dispersed precipitates and proximate phases with different lattices and plasticities, are detrimental to the high temperature ductility.

It was shown, that complex interrelationships between internal parameters weaken the material. The extend of this impairment can be amplified or mitigated by external parameters. For this reason, the possibilities of setting individual CC process parameters for crack-sensitive steels were discussed.

The precipitation kinetics can be understood by use of the institutes' slow solidification furnace, since an extremely large particle size is obtained. For high Mn steel grades, nucleation and growth of AlN and MnS precipitates became apparent.

Adaptation of the process to the material and reduction of defects are continuous challenges and need a deep understanding of multiple influences. In this context prediction of the high temperature mechanical behavior based on thermodynamic and mathematical modeling of the ductility, together with experiments and computation of solidification can support adjusting the CC process.

Acknowledgements

During his research activities in more than 25 years at the steel institute IEHK, Prof. Bleck was, despite focusing on steel design and treatment, keen in creating steel grades with extraordinary properties. The authors acknowledge gratefully the financial support of the Deutsche Forschungsgemeinschaft (DFG) within the Collaborative Research Center (SFB) 761 "Steel - ab initio; quantum mechanics guided design of new Fe based materials" and RFCS-project 800644 – PMAPIA "Precipitation of Micro Alloy Particles in B and Mn alloyed steel grades and their InterAction between elements, segregation, and defects during continuous casting". The authors thanks for the cooperation and provision of sample material to several steelmaking companies.

Open access funding enabled and organized by Projekt DEAL.

Conflict of Interest

The authors declare no conflict of interest.

Keywords

chemical steel composition, continuous casting, cracks, hot ductility, metallurgy, precipitates, segregations

Received: May 31, 2021

Revised: July 15, 2021

Published online: October 23, 2021

[1] A. Guillet, S. Yue, M. G. Akben, *ISIJ Int.* **1993**, 33, 413.

[2] M. B. Santillana, *Thermo-mechanical properties and cracking during solidification of thin slab cast steel*, Technische Universität, Delft **2013**.

[3] C. Bernhard, H. Hiebler, M. M. Wolf, *ISIJ Int.* **1996**, 36, 163.

- [4] D. N. Crowther, M. J. W. Green, P. S. Mitchell, *MSF* **1998**, 284, 469.
- [5] W. T. Lankford, *Metall. Mater. Trans. B* **1972**, 3, 1331.
- [6] K. Yasumoto, Y. Maehara, T. Nagamichi, H. Tomono, *ISIJ Int.* **1989**, 29, 933.
- [7] P. G. Krajewski, *Experimentelle Simulation der Rissbildung im Temperaturbereich des zweiten Duktilitätsminimums von Stählen*, Montanuniversität Leoben, Leoben **2013**.
- [8] L. E. Cepeda, J. M. Rodríguez-Ibabe, J. J. Urcola, M. Fuentes, *Mater. Sci.-Technol. Lond.* **1989**, 5, 1191.
- [9] S. S. Xie, J. D. Lee, U.-S. Yoon, C. H. Yim, *ISIJ Int.* **2002**, 42, 708.
- [10] K. Schwerdtfeger, *Rissanfälligkeit von Stählen beim Stranggießen und Warmumformen*, Stahleisen, Düsseldorf **1994**.
- [11] D. N. Crowther, in *The Use of Vanadium in Steel—Proceedings of the Vanitec Symposium*, Vanitec, Beijing, China, October **2001**, pp. 99–131.
- [12] M. Suzuki, Y. Yamaoka, *Mater. Trans.* **2003**, 44, 836.
- [13] E. Schmidtmann, L. Pleugel, *Archiv für das Eisenhüttenwesen* **1980**, 51, 49.
- [14] K.-h. Kim, T.-J. Yeo, K. H. Oh, D. N. Lee, *ISIJ Int.* **1996**, 36, 284.
- [15] Y. M. Won, T.-J. Yeo, D. J. Seol, K. H. Oh, *Metall. Mater. Trans. B* **2000**, 31, 779.
- [16] H. Mizukami, A. Yamanaka, T. Watanabe, *ISIJ Int.* **2002**, 42, 964.
- [17] F. Weinberg, *Metall. Trans. B* **1979**, 10, 219.
- [18] C. Olivier, C. Yvan, B. Michel, *J. Eng. Mater. Technol.* **2008**, 130, 021018.
- [19] Y. Lu, L. N. Bartlett, R. J. O'Malley, *Int. J. Met.* **2021**, 9, 836.
- [20] K. R. Carpenter, R. Dippenaar, C. R. Killmore, *Metall. Mater. Trans. A* **2009**, 40, 573.
- [21] G. A. Wilber, R. Batra, W. F. Savage, W. J. Childs, *Metall Trans A* **1975**, 6, 1727.
- [22] D. N. Crowther, Z. Mohamed, B. Mintz, *ISIJ Int.* **1987**, 27, 366.
- [23] B. Mintz, J. M. Arrowsmith, *Metals Technology* **1979**, 6, 24.
- [24] G. Alvarez de Toledo, S. Münch, T. Brune, B. Stewart, J. Komenda, *Influence of Composition and Continuous Casting Parameters on the Precipitation of Microalloyed Particles of B Microalloyed Steel Grades and Mn Alloyed Steel Grades (PMAP)*, Publications Office of the European Union, Luxembourg **2017**.
- [25] T. Brune, D. Senk, R. Walpot, B. Steenken, *Metall. Mater. Trans. B* **2015**, 46, 1400.
- [26] L. Borrmann, D. Senk, B. Steenken, J. L. L. Rezende, *Steel Res. Int.* **2020**, 22, 2000346.
- [27] R. Flesch, W. Bleck, *Steel Res.* **1998**, 69, 292.
- [28] E. Schmidtmann, F. Rakoski, *Archiv für das Eisenhüttenwesen* **1983**, 54, 357.
- [29] B. Mintz, *Ironmak Steelmak* **2000**, 27, 343.
- [30] N. E. Hannerz, *ISIJ Int.* **1985**, 25, 149.
- [31] W. A. Tiller, K. A. Jackson, J. W. Rutter, B. Chalmers, *Acta Metallurgica* **1953**, 1, 428.
- [32] A. Scholes, *Ironmak Steelmak* **2005**, 32, 101.
- [33] L. Zou, J. Zhang, Q. Liu, F. Zeng, J. Chen, M. Guan, *Metals* **2019**, 9, 1312.
- [34] P. Stadler, K. Hagen, P. Hammerschmidt, K. Schwerdtfeger, *Stahl und Eisen* **1982**, 102, 451.
- [35] J. A. Dantzig, M. Rappaz, *Solidification*, EPFL Press, Lausanne **2009**.
- [36] W. Kurz, D. J. Fisher, *Fundamentals of Solidification*, Trans Tech Publ, Uetikon-Zuerich **2005**.
- [37] K. Dou, Z. Yang, Q. Liu, Y. Huang, H. Dong, *High Temp. Mater. Process.* **2017**, 36, 741.
- [38] J. H. Hollomon, L. D. Jaffe, D. C. Buffum, *JAP* **1947**, 18, 780.
- [39] J. Platl, H. Leitner, C. Turk, R. Schnitzer, *Steel Res. Int.* **2020**, 91, 2000063.
- [40] S. K. Choudhary, A. Ghosh, *ISIJ Int.* **1994**, 34, 338.
- [41] D. Jiang, W. Wang, S. Luo, C. Ji, M. Zhu, *Metall. Mater. Trans. B* **2017**, 48, 3120.
- [42] K. Ayata, T. Mori, T. Fujimoto, T. Ohnishi, I. Wakasugi, *ISIJ Int.* **1984**, 24, 931.
- [43] W. Wang, *Simulation des Erstarrungsprozesses und des Inline-Walzens von im Strang gegossenen Stahlknüppeln mit flüssigem Kern*, RWTH Aachen University, Aachen **2006**.
- [44] P. Sivesson, G. Hallen, B. Widell, *Ironmak Steelmak* **1998**, 25, 239.
- [45] R. Thome, K. Harste, K.-J. Richter, G. Ney, *Stahl und Eisen* **2012**, 132, 61.
- [46] R. Abushosha, O. Comineli, B. Mintz, *Mater. Sci. Technol.* **1999**, 15, 278.
- [47] O. Comineli, R. Abushosha, B. Mintz, *Mater. Sci. Technol.* **1999**, 15, 1058.
- [48] T. Kizu, T. Urabe, *ISIJ Int.* **2009**, 49, 1424.
- [49] H. Hamadou, *Experimentelle und numerische Makro- und Mikromodellierung der Strukturentwicklung beim Stranggießen von Stahl*, Zugl., Dissertation, RWTH Aachen, Shaker, Aachen, **2006**.
- [50] B. Steenken, J. L. L. Rezende, D. Senk, *Mater. Sci. Technol. Lond.* **2017**, 33, 567.
- [51] E. T. Turkdogan, *Fundamentals of Steelmaking*, The Institute of Materials, London **1996**.
- [52] H. Jacobi, in *Metallurgie des Stranggießens: Giessen und Erstarren von Stahl* (Ed.: K. Schwerdtfeger), Stahleisen, Düsseldorf **1992**, pp. 125–170.
- [53] B. Mintz, A. Tuling, A. Delgado, *Mater. Sci. Technol.* **2003**, 19, 1721.
- [54] D. Senk, G. L. Thompson, P. Vicente, W. Bleck, R. Kopp, R. Steffen, ECSC-Report no. 7210-CA-834, **2000**.
- [55] R. A. Hardin, C. Beckermann, *Metall. Mater. Trans. A* **2009**, 40, 581.
- [56] R. A. Hardin, C. Beckermann, *Metall. Mater. Trans. A* **2007**, 38, 2992.
- [57] R. A. Hardin, C. Beckermann, *Metall. Mater. Trans. A* **2013**, 44, 5316.
- [58] B. G. Thomas, J. K. Brimacombe, Samarasekera I. V., *ISS Trans.* **1986**, 7, 7.
- [59] R. M. Pineda Huitron, P. E. Ramirez Lopez, E. Vuorinen, P. Nazem Jalali, M. Kärkkäinen, *ISIJ Int.* **2021**, 61, 834.
- [60] S. K. Kim, Y. D. Lee, K. Hansson, H. Fredriksson, *ISIJ Int.* **2002**, 42, 512.
- [61] E. Schmidtmann, M. Merz, *Steel Res.* **1987**, 58, 191.
- [62] E. Schmidtmann, F. Rakoski, *Archiv für das Eisenhüttenwesen* **1983**, 54, 363.
- [63] P. Bekeč, M. Longauerová, M. Vojtko, O. Milkovič, J. Kadlec, G. Tréfa, G. Grimplini, *J. Achiev. Mater. Manuf. Eng.* **2014**, 67, 58.
- [64] H. G. Suzuki, S. Nishimura, J. Imamura, Y. Nakamura, *ISIJ Int.* **1984**, 24, 169.
- [65] D. N. Crowther, B. Mintz, *Mater. Sci. Technol.* **1986**, 2, 671.
- [66] R. Abushosha, R. Vipond, B. Mintz, *Mater. Sci. Technol.* **1991**, 7, 613.
- [67] K. M. Banks, A. Tuling, B. Mintz, *J. South Afr. Inst. Min. Metall.* **2011**, 111, 711.
- [68] E. López-Chipres, I. Mejía, C. Maldonado, A. Bedolla-Jacuinde, J. M. Cabrera, *Mater. Sci. Eng., A* **2007**, 460, 464, <https://www.sciencedirect.com/science/article/pii/S0921509307001591>.
- [69] K. Unterberg, *Einfluss der Legierungszusammensetzung auf die mittels Heißzugversuchen bestimmten Hochtemperatüreigenschaften*, RWTH Aachen University, Aachen **2019**.
- [70] C. Fix, D. Senk, in *Proc.—METEC & 4th ESTAD*, Steel Institute VDEh, Düsseldorf **2019**.
- [71] D. Senk, *presented at 9th ECCS*, Vienna, Austria **2017**.
- [72] A. von Könemann, *Untersuchung des Einflusses von Aluminium auf das Erstarrungsgefüge bei gleichgewichtsnaher Erstarrung im System Fe-Mn-C-Al*, RWTH Aachen University, **2016**, unpublished.
- [73] M. Vynnycky, *J. Math. Ind.* **2020**, 10, 217.
- [74] F. Oeters, *Metallurgie der Stahlherstellung*, Verlag Stahleisen, Düsseldorf **1994**.
- [75] R. Boom, A. A. Kamperman, O. Dankert, A. van Veen, *Metall. Mater. Trans. B* **2000**, 31, 913.

- [76] H. Yang, S. P. Vanka, B. G. Thomas, *JOM* **2018**, 70, 2148.
[77] J. Campbell, in *Complete Casting Handbook*, Elsevier, Amsterdam **2015**, pp. 341–415.
[78] T. S. Piwonka, M. C. Flemings, *Trans. Metall AIME* **1996**, 236, 1157.
[79] T. Edvardsson, H. Fredriksson, I. Svensson, *Met. Sci.* **1976**, 10, 298.
[80] G. K. Sigworth, C. Wang, *Metall. Trans. A* **1993**, 24, 349.
[81] T. Brune, K. Kortzak, D. Senk, N. Reuther, M. Schäperkötter, in *ASMET (Hg.) 2014 – 8th ECCC*, ASMET, Graz, Austria, pp. 792–801.



Dieter Senk dedicated his life to iron and steel technology and science. Born in 1957, he studied at the TU Clausthal (Germany), where he also got his doctoral degree. For 15 years, he worked on the development of direct strip casting processes at Thyssen Steel Company. In 2001, he was appointed as professor for the chair of iron and steel metallurgy at the RWTH Aachen University where he expanded his research on iron ore reduction processes and the development of shaft furnaces. By carrying out R&D-projects and lecturing on iron and steel making, he contributes to both science and education.